

## **Analysis of Deprotection Reaction in Chemically Amplified Resists Using an Fourier Transform Infrared Spectrometer with an Exposure Tool**

**Atsushi Sekiguchi, Yasuhiro Miyake and Mariko Isono**

**Litho Tech Japan Corp., 2-6-6-201 Namiki, Kawaguchi, Saitama 332-0034, Japan**

(Received September 28, 1999 accepted December 2, 1999)

The reaction of dissociation of protection groups (hereafter the "deprotection reaction") was observed *in situ* during exposure of chemically amplified resists using an FT-IR spectrometer equipped with an exposure unit, at a wavelength of 248 nm. The deprotection reaction in the chemically amplified resists during exposure was modeled on the basis of the *in situ* IR measurement results, and the deprotection reaction constant  $C_2$ , reaction initiation delay constant  $E_0$ , and average acid lifetime constant  $\tau_2$  were calculated. Herein, we report our results. The chemically amplified resists used in the experiments were based on polystyrene (PS) and had a t-butoxycarbonyl (t-BOC) protection group (hereafter "t-BOC resist") and a 1-ethoxyethyl (ethyl acetal) resist (hereafter "EA resist"). The deprotection reaction in the t-BOC resist was observed through changes in the infrared spectrum at 1150  $\text{cm}^{-1}$  (C-O ester bonds); the deprotection reaction in the EA resist was monitored through changes in the infrared spectrum at 2980  $\text{cm}^{-1}$  (H-C-H alkane bonds). It was found that at room temperature (23°C), whereas the deprotection reaction in the t-BOC resist during exposure occurred to the extent of only 5% complete, it occurred nearly to completion in the EA resist. The change in absorption with exposure time was converted into a protection ratio for protection groups, and fitted to a newly devised deprotection reaction model to estimate the deprotection reaction parameters for exposure. The deprotection reaction parameters thus obtained were input in to a profile simulator, and profile simulations were attempted. The results indicated that whereas the t-BOC resist could be patterned at an ambient a temperature of 70°C and above during exposure, the EA resist could be patterned at room temperature. In resist development and studies of resist processes, this system is expected to prove useful for the analysis of deprotection reactions during exposure.

**KEYWORDS:** chemically amplified resist, deprotection reaction, protection groups, FT-IR spectrometer, activation energy, lithography simulation

## 1. Introduction

Beginning with the research by Ito et al. in 1984[1], chemically amplified resists using acid catalysts have now become indispensable for the manufacture of semiconductor devices at sub-half-micron and lower levels. Since this early work referred to above, a number of studies have been conducted on the improvement of resolution of chemically amplified resists, their stability in different environments, and other related subjects[2]~[5]. Positive-type chemically amplified resists use a photochemical reaction to generate acid, and in the heating process following the exposure (post-exposure baking, PEB) this acid acts as a catalyst to dissociate protection groups. Consequently, in addition to the efficiency of acid generation by exposure and acid diffusion, the types of protection groups, protection ratio and other factors are closely related to the resist performance. An accurate understanding of the deprotection reaction is essential for resist development and process evaluations. In recent years, a number of models have been proposed[6]~[8] as being appropriate to describe deprotection reactions during PEB, and progress in the analysis has been made, but there have not yet been any reports on analysis of the deprotection reactions during exposure. We therefore constructed an Fourier transform infrared (FT-IR) spectrometer equipped with an exposure tool, and developed a system for the analysis of deprotection reactions in positive-type chemically amplified resists during exposure. Using this system, we performed *in situ* observations of deprotection reactions in chemically amplified resists during exposure, and developed a model of deprotection reactions in such resists during exposure, which we describe below. We also calculated the deprotection reaction constant  $C_2$  during exposure, the reaction initiation delay constant  $E_0$ , and the average acid lifetime constant  $\tau_2$ , and used these results in profile simulations, also reported here.

## 2. Hardware Configuration

An external view of the equipment appears in Figure 1. Bio-Rad's model FTS-135 was used as the FT-IR spectrometer. Ultraviolet rays from a Xe-Hg lamp are reduced by a narrow band filter to a narrow wavelength band centered at 248 nm (width at half-maximum 12 nm), and the radiation passes through an optical fiber to irradiate a wafer. The luminosity at the irradiated surface is 1 mW/cm<sup>2</sup>. To control the

temperature of the exposure environment, a temperature control plate is positioned perpendicularly to the optical measurement path. By cooling or heating the temperature control plate, the temperature of the exposure environment can be varied between  $-3^{\circ}\text{C}$  and  $150^{\circ}\text{C}$ . Measurements were performed in transmissive mode. A 10 mm diameter hole was opened in the center of the temperature control plate, a wafer transport shuttle was used to transport the wafer onto the plate, and after the wafer had reached the desired temperature, IR measurements were performed simultaneously with UV irradiation. In order to eliminate the effect of  $\text{CO}_2$  in the air, aluminum tubing was used to shield the measurement optical path and  $\text{N}_2$  purging was performed in order to reduce the amount of noise in the measurements.

### 3. Experimental Procedure and Results

#### 3.1 Experimental conditions

The structures of the resists studied in this work appear in Figure 2. Positive-type chemically amplified resists based on polystyrene and protected by t-butoxycarbonyl (t-BOC) and 1-ethoxyethyl (ethyl acetal) groups were prepared. Protection rates were 30% for the t-BOC resist and 20% for the EA resist; the Photo Acid Generator (PAG) was impregnated with triphenyl sulphonium triflate (TPS) at a 3% resin ratio. No quenchers were added to either resist. A silicon substrate was coated with these resists to a thickness of  $0.7\ \mu\text{m}$ , and *in situ* IR measurements were performed during exposure. Prebaking was performed at  $90^{\circ}\text{C}$  for 60 sec for both cases.

#### 3.2 Experimental results

Figure 3 presents results of *in situ* IR measurements of the t-BOC resist during exposure and PEB. Exposure time and PEB time elapse with moving from the back to the front of the graph. The horizontal axis represents the wave number ( $\text{cm}^{-1}$ ); the vertical axis indicates the absorption. IR measurements were performed over the wave number range of 500 to  $4000\ \text{cm}^{-1}$ , with a resolution of  $4\ \text{cm}^{-1}$ . A single measurement scan was performed, with sampling every two seconds.

Observations of deprotection reactions in the t-BOC resist are based on changes in the  $1150\ \text{cm}^{-1}$  absorption peak of C-O (ester) bonds accompanying the deprotection. Figure 3(a) shows the *in situ* IR measurement results during exposure at room temperature ( $23^{\circ}\text{C}$ ). A slight decrease in the ester bond absorption peak can be seen. Figure 3(b) shows the results of *in situ* IR measurements during PEB, after exposure at  $180\ \text{mJ}/\text{cm}^2$  (following the exposure represented in Figure 3(a)). As PEB is begun, the deprotection reaction proceeds rapidly. Thus in the t-BOC resist, the

deprotection reaction is minimal at room temperature (23°C) during exposure, but with PEB, it proceeds significantly more rapidly.

Figure 4 similarly presents the results of *in situ* IR measurements for the EA resist during exposure and PEB. Observation of deprotection reactions in the EA resist are based on changes in the 2980 cm<sup>-1</sup> absorption peak of H-C-H (alkane) bonds accompanying the deprotection. Other measurement conditions are the same as for the t-BOC resist. Figure 4(a) shows the *in situ* IR measurement results during exposure at room temperature (23°C). It can be seen that the alkane bond absorption peak decreases drastically with exposure. The results of *in situ* IR measurements during the subsequent PEB, following exposure at 80 mJ/cm<sup>2</sup>, appear in Fig. 4(b). Exposure causes nearly complete disappearance of alkane bond absorption, and the slight amount of alkane bond absorption remaining is eliminated by PEB. From these results, it was determined that the deprotection reaction in the EA resist at room temperature (23°C) runs to 95% completion during exposure, and the few remaining protection groups are dissociated by the subsequent PEB.

Figure 5 illustrates the schemes of the deprotection reactions during exposure proposed for each of these resists on the basis of the observations of the deprotection reaction during exposure. In the t-BOC resist, an acid is generated by exposure, and it is thought that an acid-catalyzed reaction causes tertiary butoxycarbonyl groups to be dissociated, with the production of polyhydroxystyrene, and its decomposition into carbonic acid gas and isobutene. On the other hand, in the EA, resist exposure produces acid, and an acid-catalyzed reaction causes dissociation of the ethyl acetal groups, with the production of polyhydroxystyrene; the dissociated ethyl vinyl ether undergoes hydrolysis and resulting in its decomposition into ethanol and aldehyde.

#### 4. Calculation Model and Data Analysis

Taking as reference the absorption spectrum measured under conditions of complete dissociation of the protection groups upon exposure at sufficient radiation energies and PEB, the absorption spectra measured under various exposure conditions were normalized and converted into protection group concentrations. By applying the equation below of Ohfuji's model[7] for the deprotection reactions during exposure to the relation thus obtained between the protection rate and exposure energy, we have adopted a new model equation, which adds to Ohfuji's model the effect of reaction delay and that of the average acid lifetime constant during exposure. The deprotection reaction parameters related to the deprotection reaction during exposure can be determined.

$$[P]_{\text{exp}} = \exp\left\{-C_2 \cdot \frac{(E - E_0)}{\tau_2}\right\} \quad (1)$$

Here,  $[P]_{\text{exp}}$  is the normalized protection rate on exposure,  $C_2$  is the deprotection reaction constant during exposure,  $E_0$  is the reaction delay constant,  $\tau_2$  is the average acid lifetime constant during exposure, and  $E$  is the exposure energy ( $\text{mJ}/\text{cm}^2$ ).

A final deprotection model valid for both exposure and PEB, incorporating the deprotection reaction model in PEB reported in ref. [8], is expressed by eq. (2).

$$[P] = [P]_{\text{exp}} \bullet [P]_{\text{PEB}} \quad (2)$$

where

$$[P]_{\text{PEB}} = \exp\left[-K_{dp} [H]^m \left\{1 - \exp\left(-\frac{m(t - T_d)}{\tau_1}\right)\right\} \frac{\tau_1}{m}\right] \quad (3)$$

$$[H] = 1 - \exp(-C_1 E) - Q$$

Here,  $[P]$  is the final normalized protection rate for protection groups after exposure and PEB,  $K_{dp}$  is the deprotection reaction constant during PEB ( $\text{s}^{-1}$ ),  $m$  is the deprotection reaction order in PEB,  $t$  is the PEB time,  $C_1$  is the reaction constant ( $\text{cm}^2/\text{mJ}$ ) on PAG exposure,  $E$  is the exposure energy ( $\text{mJ}/\text{cm}^2$ ),  $Q$  is the quencher constant,  $T_d$  is the reaction delay constant in PEB, and  $\tau_1$  is the average acid lifetime constant in PEB.

An example of fitting of eq. (1) for the t-BOC resist at an exposure environment temperature of  $50^\circ\text{C}$  appears in Figure 6. The plotted data are measured values, and the line is the best-fit result. There is good agreement between the measurements and fitting results. We then performed *in situ* IR measurements at different exposure environment temperatures for the two resists, and calculated the deprotection parameters at each temperature (Figure 7). Figure 7(a) shows the best-fit results for the t-BOC resist at 8, 23, 40, 60, and  $100^\circ\text{C}$ . While there is some deviation at  $100^\circ\text{C}$ , overall good agreement between the measurements and results from the model is obtained. Figure 7(b) similarly shows the fitting results for the EA resist at -2.5, 8, 23, 40, 60, and  $100^\circ\text{C}$ . As with the t-BOC resist, some deviation is seen at  $100^\circ\text{C}$ ,

but the EA resist also yields good agreement between measurements and results from the model. Comparison of the deprotection reactions during exposure at room temperature reveals that, whereas the reaction is only about 5% complete in the t-BOC resist even after exposure at 600 mJ/cm<sup>2</sup>, in the EA resist the reaction runs nearly to completion on exposure at approximately 60 mJ/cm<sup>2</sup>.

The exposure deprotection reaction constants obtained appear in Table I. The reaction delay constant  $E_0$  was essentially 0 for both resists at all temperatures, indicating that the deprotection reaction takes place simultaneously with the start of exposure in both the t-BOC resist and the EA resist, regardless of the temperature. The acid lifetime during exposure,  $\tau_2$ , was also nearly 1 at all temperatures, indicating that the acid generated by TPS has a long lifetime in the polymer in both resists, regardless of the exposure temperature.

Figure 8 shows the Arrhenius plots of the deprotection reaction constant during exposure,  $C_2$ . The plots for both resists reveal two rate-limiting regions. One is in the low-temperature region, corresponding to a high activation energy; the other is in the high-temperature region with a low activation energy. It is reported that in deprotection reactions during PEB, the step determining the reaction rate is limited by acid diffusion at high temperatures, and by the deprotection reaction at low temperatures[9]–[10]. For the case of deprotection reactions during exposure, similar conclusions were made. It was confirmed that reaction regions with different thresholds exist at 50°C in the t-BOC resist, and at 20°C in the EA resist. Table II shows the activation energies of the deprotection reactions during exposure as calculated from the Arrhenius plots. Whereas the activation energy ( $E_a$ ) of the t-BOC resist at room temperature is 25.1 kcal/mol, that for the EA resist is 3.15 kcal/mol. Thus the activation energy of the EA resist is significantly lower than that of the t-BOC resist, therefore, the deprotection reaction can be expected to occur readily at room temperature. Table III shows the frequency factors.

Figure 9 compares the discrimination curves for samples exposed at room temperature, with and without PEB. If the t-BOC resist is not subjected to PEB, adequate dissolution discrimination is not obtained even if the exposure dose is increased. On the other hand, dissolution discrimination sufficient for pattern resolution is obtained for the EA resist, even without PEB. Thus, the results of this analysis are in good agreement with the actual contrast of development, suggesting the validity of the method used for the analysis.

## 5. Simulation

The deprotection model during exposure presented above [eq. (1)] was incorporated into simulations[11], and profile simulations of the deprotection reaction during exposure were conducted. Table IV shows the simulation conditions.

The optical and development parameters used in the simulations were values measured using an ABC analyzer, model ABC-400[12] and a Resist Development Analyzer, model RDA-790[13], both manufactured by Litho Tech Japan. The measured values are indicated below. Development parameters were measured for samples subjected to PEB at 120°C for 60 s. Table V shows the development parameters for both resists.

Figure 10 presents the results of resist simulations for the t-BOC and EA resists at different exposure at ambient temperatures. Exposure doses were 7.0 mJ/cm<sup>2</sup> for the t-BOC resist and 1.73 mJ/cm<sup>2</sup> for the EA resist. The simulation results reveal that when PEB is not performed after exposure at 25°C, near room temperature, there is almost no pattern resolution in the t-BOC resist, whereas the pattern is resolved in the EA resist, in good agreement with the results of observations of the deprotection reaction during exposure at room temperature using the system described above. This tends to confirm the validity of the model of the deprotection reaction during exposure presented by us in this paper. The simulations also verified that patterning is possible by exposure at ambient temperatures of 70°C or higher in the case of the t-BOC resist, and 15°C or higher in the case of the EA resist.

## 6. Conclusion

An FT-IR spectrometer equipped with an exposure unit of 248 nm wavelength was used in *in situ* observations of the reaction of dissociation of protection groups in chemically amplified resists during exposure. The observation results were used to model the deprotection reactions during exposure of the chemically amplified resists, and deprotection reactions occurring during exposure in a t-BOC resist and an EA resist were analyzed. It was found during exposure that at room temperature (23°C), whereas the deprotection reaction in the t-BOC resist occurred to only about 5% completion, in the EA resist, the deprotection reaction continued essentially to completion. The changes in optical absorption by protection groups with exposure time were converted into protection group protection rates, the results were fitted to an equation proposed in this paper to model the deprotection reaction during exposure, and the deprotection reaction parameters were estimated. In addition, the activation energies for both the resists as determined by the Arrhenius plots of the deprotection reaction constant  $C_2$ , thus obtained were compared. The activation energy ( $E_a$ ) at room temperature for the

EA resist was 3.15 kcal/mol, low compared with that for the t-BOC resist of 25.1 kcal/mol. It was thus confirmed that the greater tendency for the deprotection reaction to occur in the EA resist as compared with the t-BOC resist during exposure at room temperature can be explained in terms of the difference in the activation energies.

The exposure deprotection reaction parameters thus obtained were input into a profile simulator, and profile simulations conducted. For exposure at room temperature (without PEB), no pattern resolution was obtained in the t-BOC resist, but pattern resolution was noted in the EA resist; this finding was in agreement with both the *in situ* IR measurement results and the results of development discrimination measurements. The agreement tends to corroborate the validity of the proposed model. This system can thus be used to accurately analyze deprotection reactions occurring during exposure. Hereafter, it will be necessary to conduct additional studies on a variety of protection groups and different PAGs in order to further elucidate the nature of the deprotection reactions occurring during exposure.

### Acknowledgements

The authors wish to thank Dr. Tomita and Mr. Kuniyoshi of the Photosensitive Materials Research Center of Toyo Gosei Kogyo for providing both materials and useful advice in the course of this research. They also wish to thank Dr. Ofuji of Intel for his useful advice relating to the modeling of the deprotection reactions.

### References

- 1) H. Ito and C. G. Willson: ASC Symp. Ser. **2** (1984) 11.
- 2) J. V. Crivello and J. H. W. Lam: *Macromolecules* **10** (1977) 1307.
- 3) R. A. Ferguson, C. A. Spence, E. Reichmanis, L. F. Thompson and A. R. Neureuther: *Proc. SPIE* **1262** (1990) 412.
- 4) G. Pawlowski, R. Dammel and C. R. Lindley: *Proc. SPIE* **1262** (1990) 16.
- 5) R. D. Allen, I. Y. Wan, G. M. Wallraff, R. A. Dipietro and D. C. Hofer: *J. Photopolym. Sci. Technol.* **8** (1995) 623.
- 6) T. Ohfuji, A. G. Timko, O. Nalamasu and D. R. Stone: *Proc. SPIE* **1925** (1993) 213.
- 7) T. Ohfuji, K. Nakano, K. Maeda and E. Hasegawa: *J. Vac. Sci. Technol.* **13** (1995) 3022.
- 8) A. Sekiguchi, C. A. Mack, M. Isono and T. Matsuzawa: *Proc. SPIE* **3678** (1999) 985.
- 9) M. Yamana, T. Itani, H. Yoshino, S. Hashimoto, N. Samoto and K. Kasama: *Proc. SPIE* **3049** (1997) 269.
- 10) M. Yamana, T. Itani, H. Yoshino, S. Hashimoto, H. Tanabe and K. Kasama: *Proc.*

SPIE **3333** (1998) 32.

- 11) C. A. Mack , M. J. Maslow, R.Carpio and A. Sekiguchi: Proc. Inter Face '97 (1997)  
p.203.
- 12) A. Sekiguchi, Y. Minami, T. Matsuzawa, T. Takezawa and H. Miyakawa:  
Electron. & Commun. Jpn. Pt. 2 **78** (1997) 21.
- 13) A. Sekiguchi, C. A. Mack, Y. Minami and T. Matsuzawa: Proc. SPIE **2725** (1996) 49.

**Table I Deprotection reaction rate constant  $C_2$ .**

**(a) t-butoxycarbonyl**

Temp.( °C)	$C_2 (\times 10^{-3})$
8	0.06
20	0.09
23	0.11
28	0.42
40	1.00
50	3.90
60	2.90
70	6.50
80	13.0
90	18.0
100	21.0
110	22.0

**(b) 1-ethoxyethyl**

Temp.( °C)	$C_2 (\times 10^{-3})$
-2.5	3.00
8	5.90
20	6.20
28	6.60
30	6.10
40	7.20
60	9.40
70	12.6
80	14.0
90	15.0
100	16.1
110	20.7
120	21.8

**Table II Activation energies of the deprotection reactions.**

Resist	(kcal/mol)	
	Low-Temperature Region	High-Temperature Region
t-Butoxycarbonyl	25.128 (3~50°C)	6.835 (50~100°C)
1-Ethoxyethyl	30.125 (-2.5~20°C)	3.148 (20~120°C)

**Table III Estimated frequency factor.**

Resist	(s <sup>-1</sup> )	
	Low-Temperature Region	High-Temperature Region
t-Butoxycarbonyl	33.58 (3~50°C)	5.25 (50~100°C)
1-Ethoxyethyl	8.92 (-2.5~20°C)	2.50 (20~120°C)

**Table IV Simulation conditions.**

<b>Exposure wavelength</b>	<b>248 nm</b>
<b>NA</b>	<b>0.63</b>
<b>Coherence factor</b>	<b>0.60</b>
<b>Lines and space</b>	<b>0.25 μm</b>
<b>Development conditions</b>	<b>NMD-3 (TMAH 2.38%), 60 s</b>
<b>Substrate</b>	<b>Si without BARC</b>

**Table V Development parameters for simulations.**

<b>Simulation parameters</b>	<b>t-BOC resist</b>	<b>EA resist</b>
<b><math>R_{\max}</math></b>	<b>39.2</b>	<b>308</b>
<b><math>R_{\min}</math></b>	<b>0.015</b>	<b>0.013</b>
<b>n</b>	<b>5.2</b>	<b>3.4</b>
<b><math>M_{th}</math></b>	<b>0.98</b>	<b>0.90</b>
<b>PAG diffusivity D (nm<sup>2</sup>/s)</b>	<b>43.5</b>	<b>46.7</b>
<b>Inhibition depth <math>\sigma</math> (nm)</b>	<b>15</b>	<b>13</b>
<b>Inhibition rate <math>R_0</math></b>	<b>0.12</b>	<b>0.10</b>
<b><math>A_{DIII}</math> (<math>\mu\text{m}^{-1}</math>)</b>	<b>0.0108</b>	<b>0.0112</b>
<b><math>B_{DIII}</math> (<math>\mu\text{m}^{-1}</math>)</b>	<b>0.559</b>	<b>0.513</b>
<b><math>C_{DIII}</math> (cm<sup>2</sup>/mJ)</b>	<b>0.011</b>	<b>0.012</b>
<b>Resist thickness (nm)</b>	<b>700</b>	<b>700</b>
<b>Pre-Bake (<math>^{\circ}\text{C}</math>, s)</b>	<b>90, 60</b>	<b>90, 60</b>
<b>PEB (<math>^{\circ}\text{C}</math>, s)</b>	<b>110, 60</b>	<b>110, 60</b>

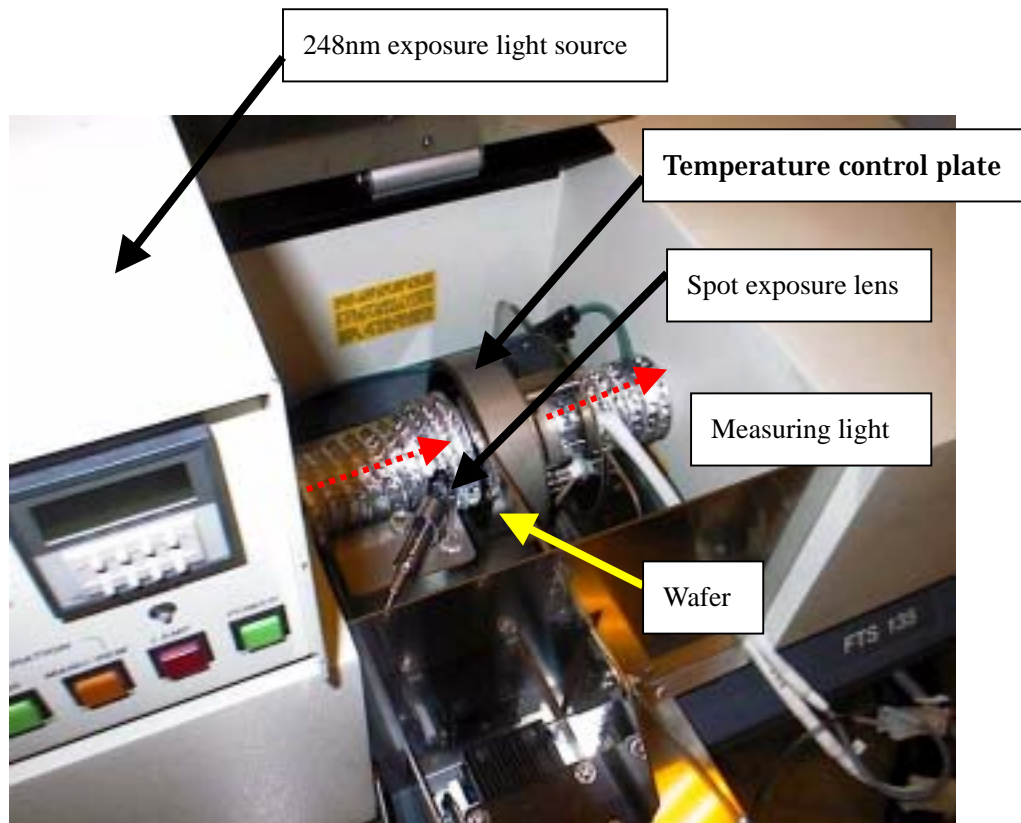


Fig.1 External view of the FT-IR measurement tool with the in situ exposure system and PEB system.

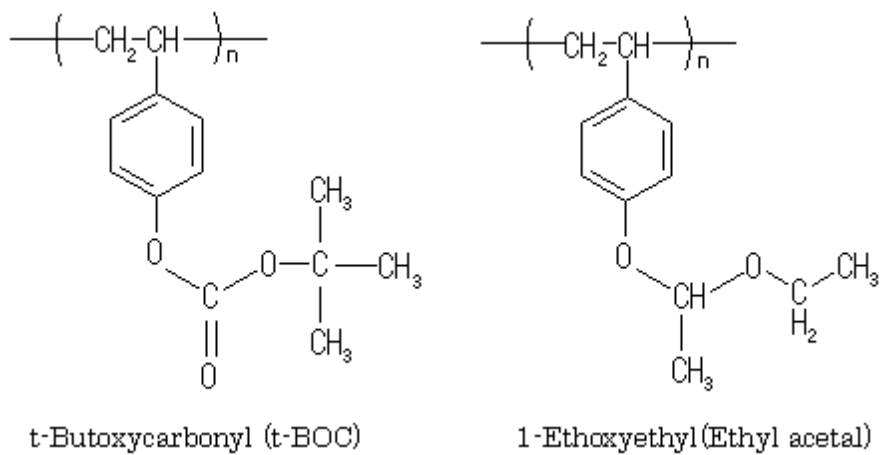
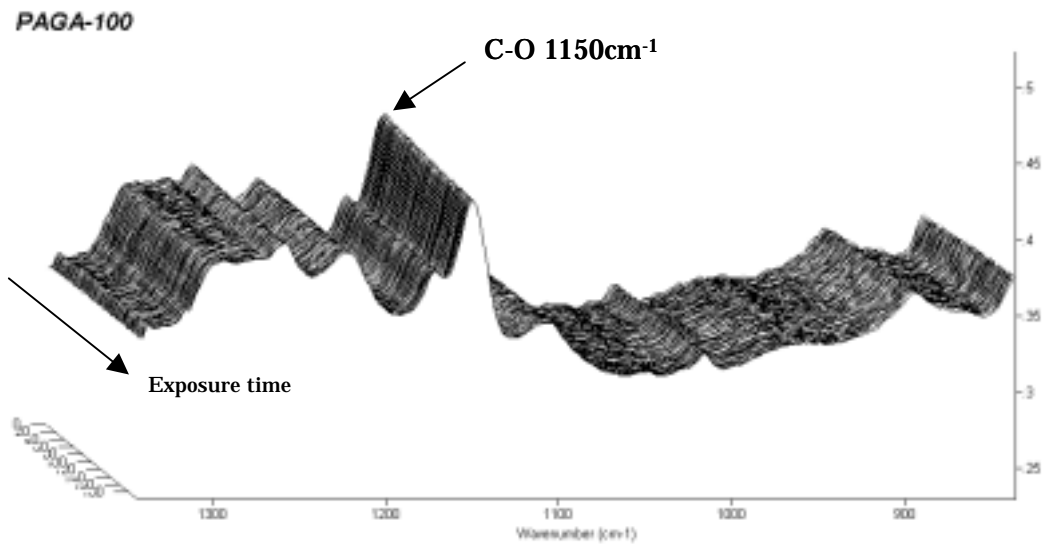
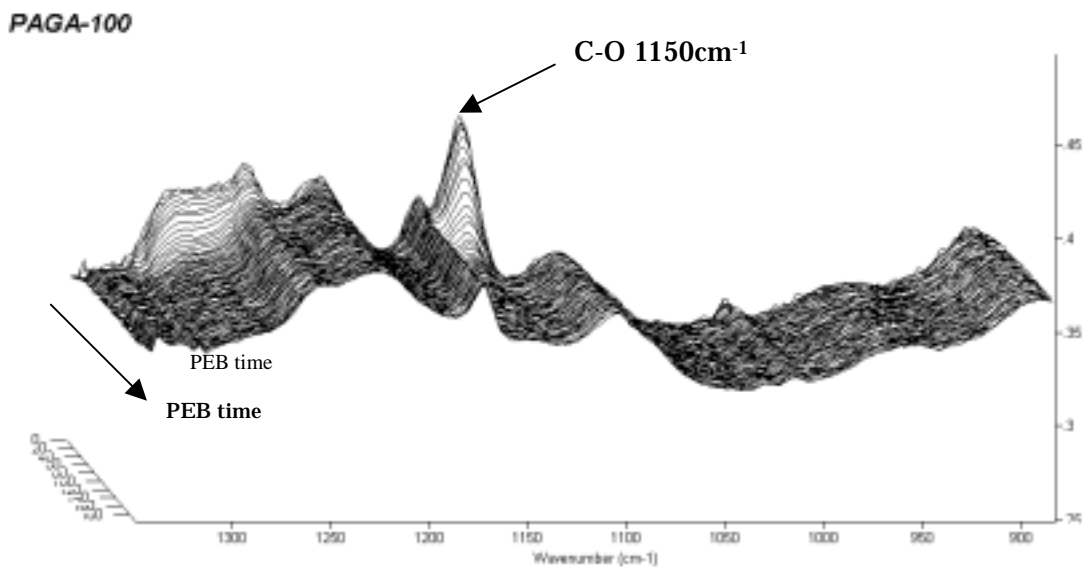


Fig.2 Chemical structure of t-butoxycarbonyl resist and 1-ethoxyethyl resist.

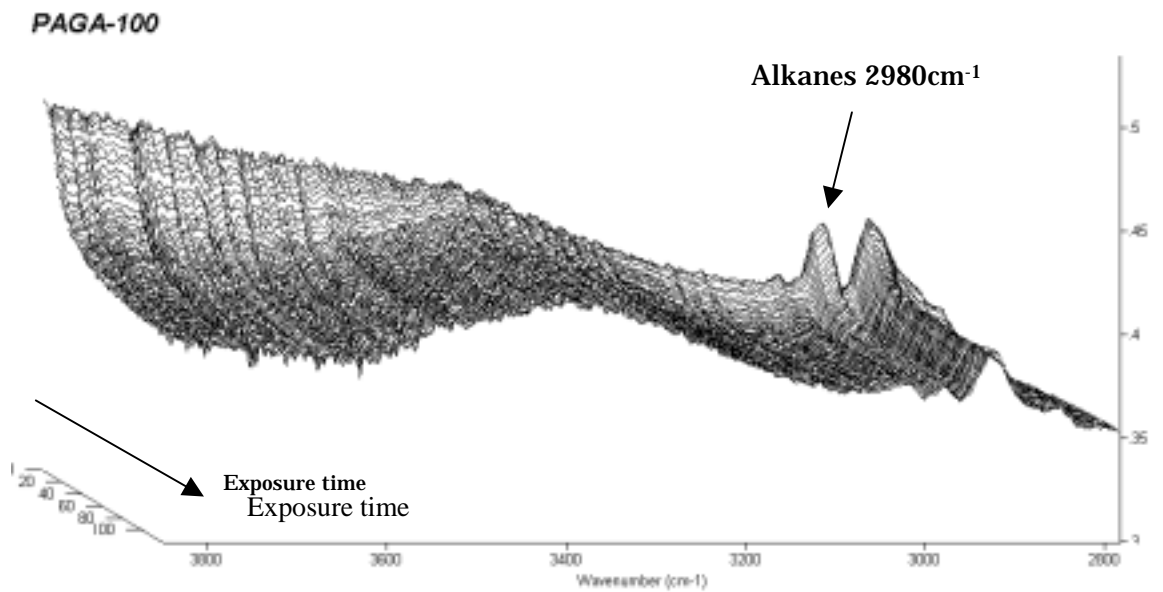


(a)

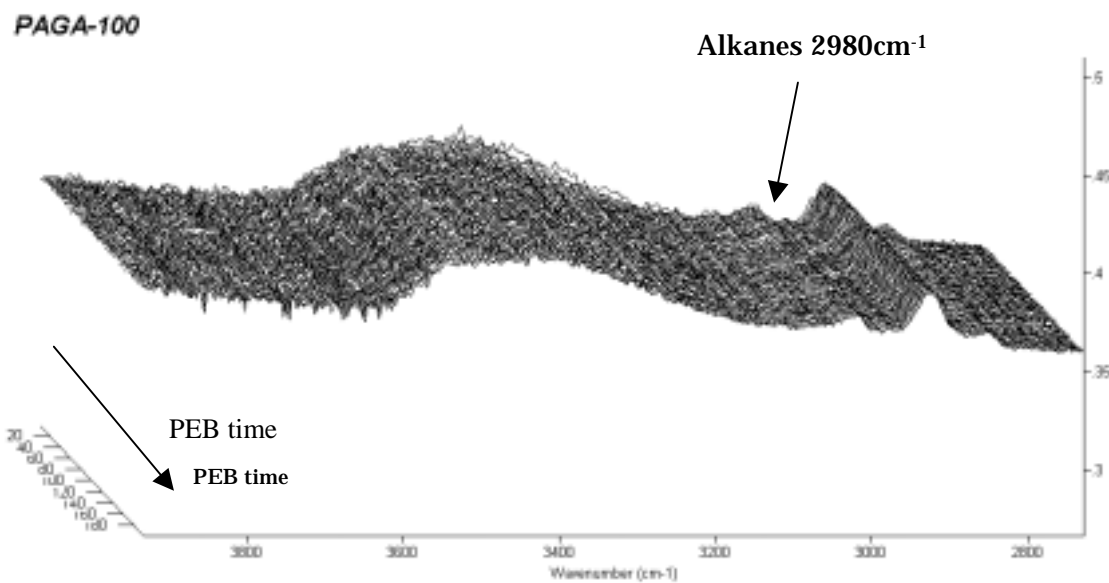


(b)

Fig.3 Typical FT-IR difference spectra showing deprotection reactions as a function of (a) the exposure time (exposed at 1mW/cm<sup>2</sup>) and, (b) the PEB time (120°C PEB temperature) the t-butoxycarbonyl resist.

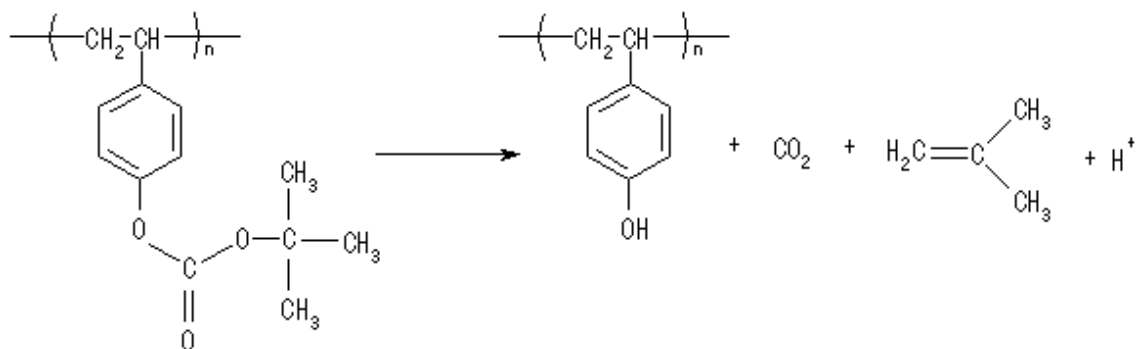


(a)

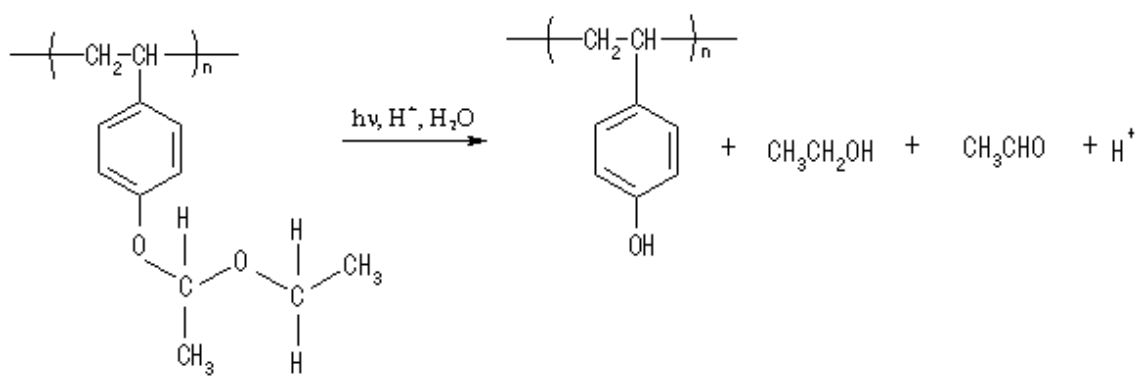


(b)

Fig.4 Typical FT-IR difference spectra showing the deprotection reaction as a function of (a) the exposure time (exposed at 1mW/cm<sup>2</sup>) and, (b) the PEB time (120°C PEB temperature) in the 1-ethoxyethyl resist.



(a)



(b)

Fig 5 Expected deprotection reactions for (a) t-butoxycarbonyl resist,  
 and (b) 1-ethoxyethyl resist during exposure.

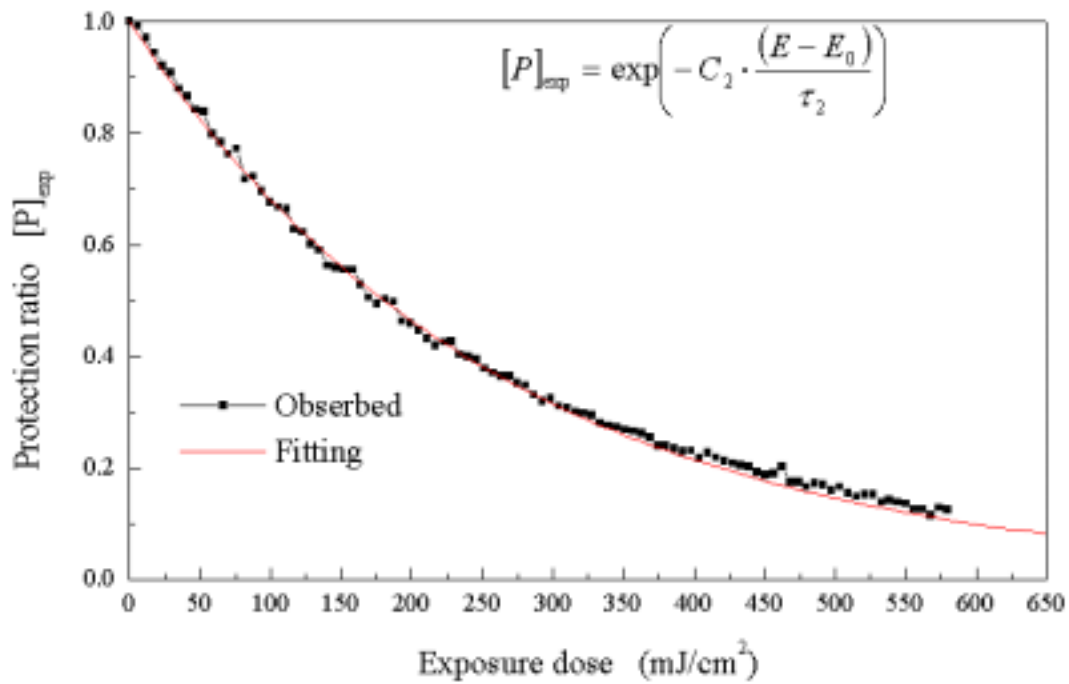
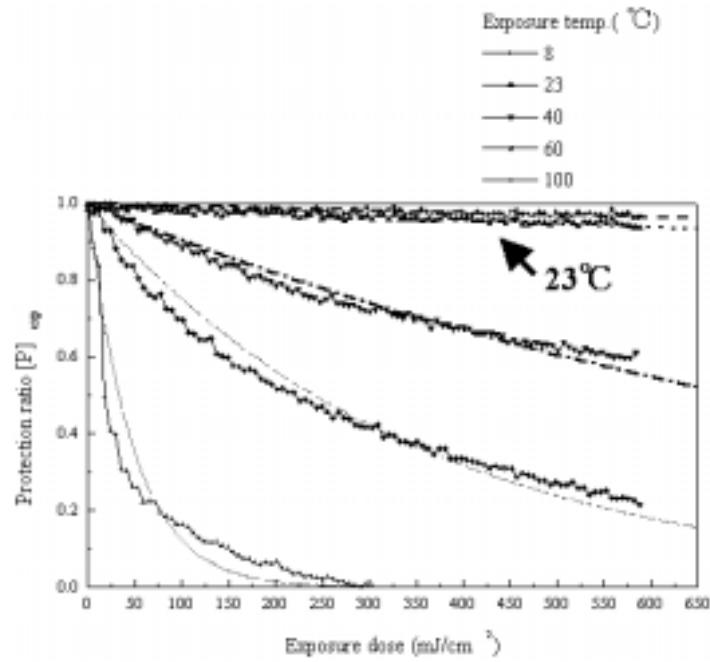
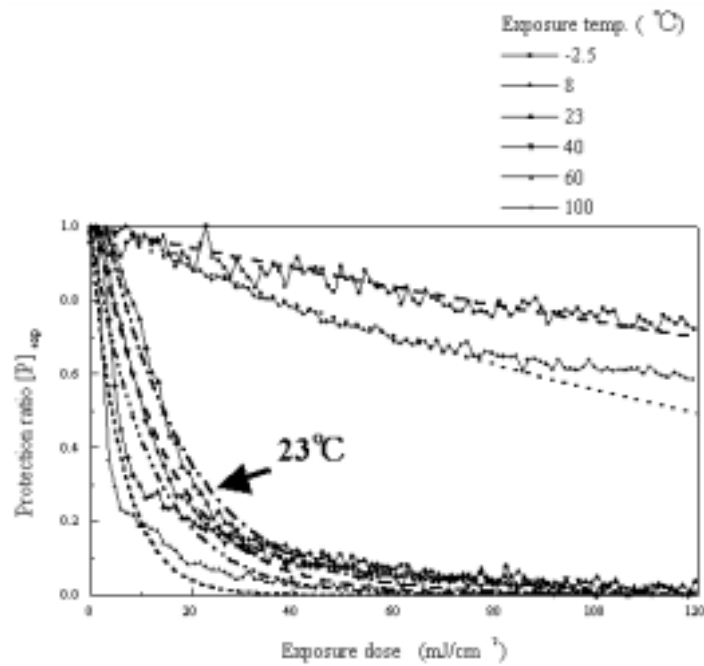


Fig.6 Normalized protection ratio calculated from the FT-IR spectra  
as a function of the exposure dose  
(t-butoxycarbonyl resist and exposure temperature 50°C).



(a)



(b)

Fig.7 Relationship between  $[P]_{exp}$  and exposure dose as a function of the exposure temperature for (a) t-butoxycarbonyl resist and, (b) 1-ethoxyethyl resist.

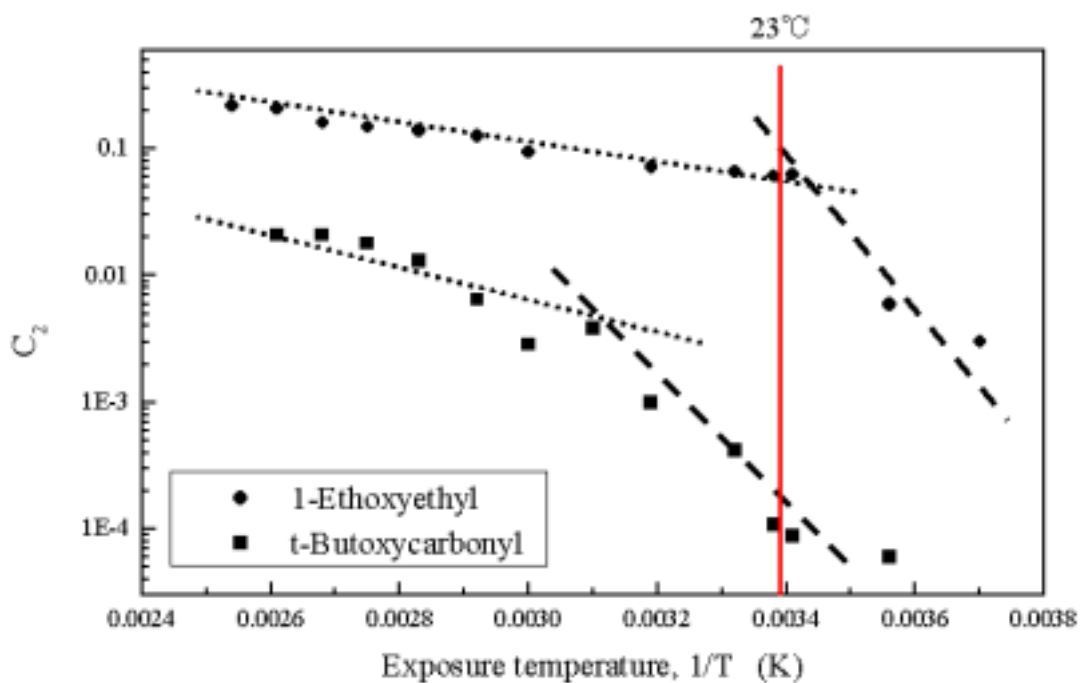
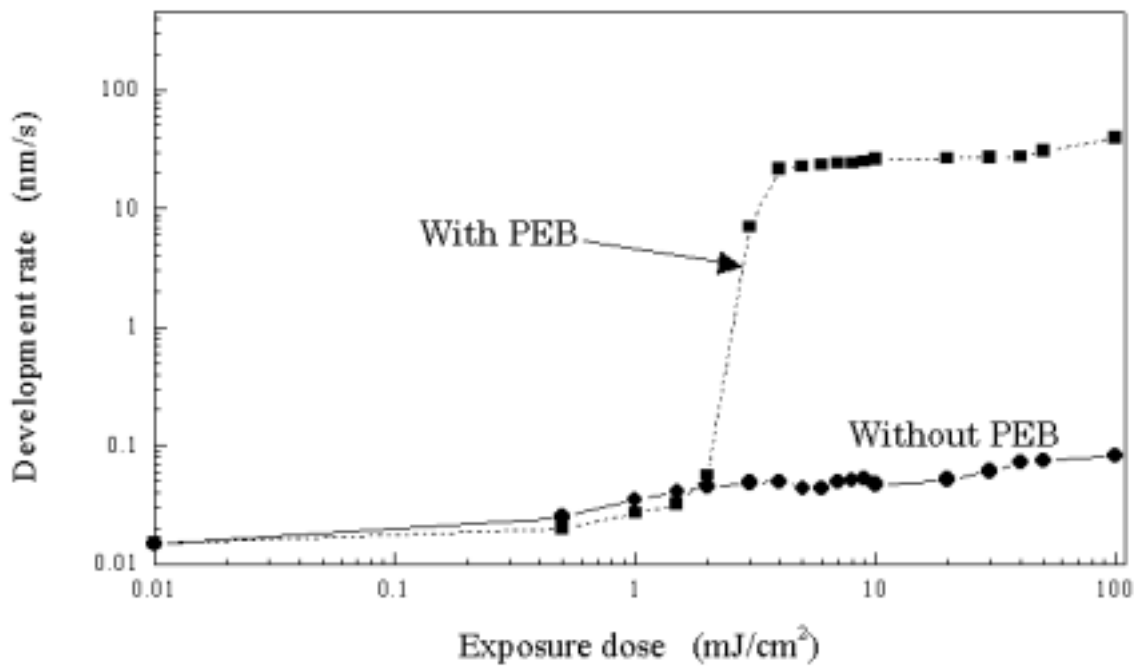
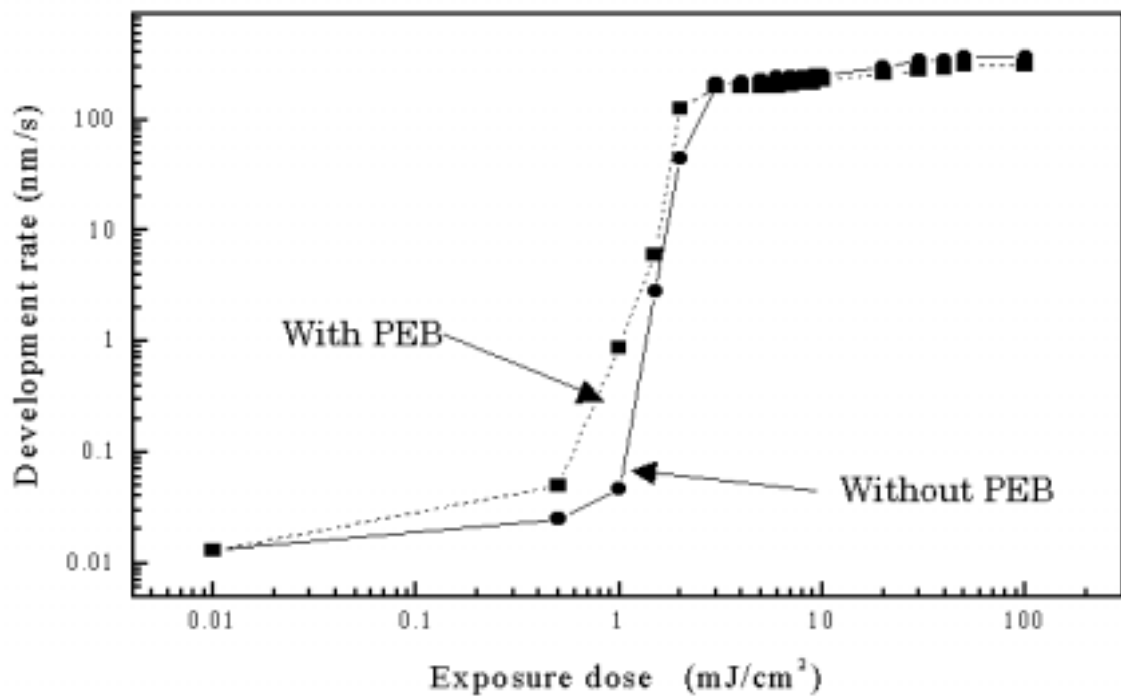


Fig. 8 Arrhenius plots of deprotection reaction rate constant  $C_2$ .



(a)



(b)

Fig.9 Discrimination curve for (a) t-butoxycarbonyl resist, and (b) 1-ethoxyethyl resist.

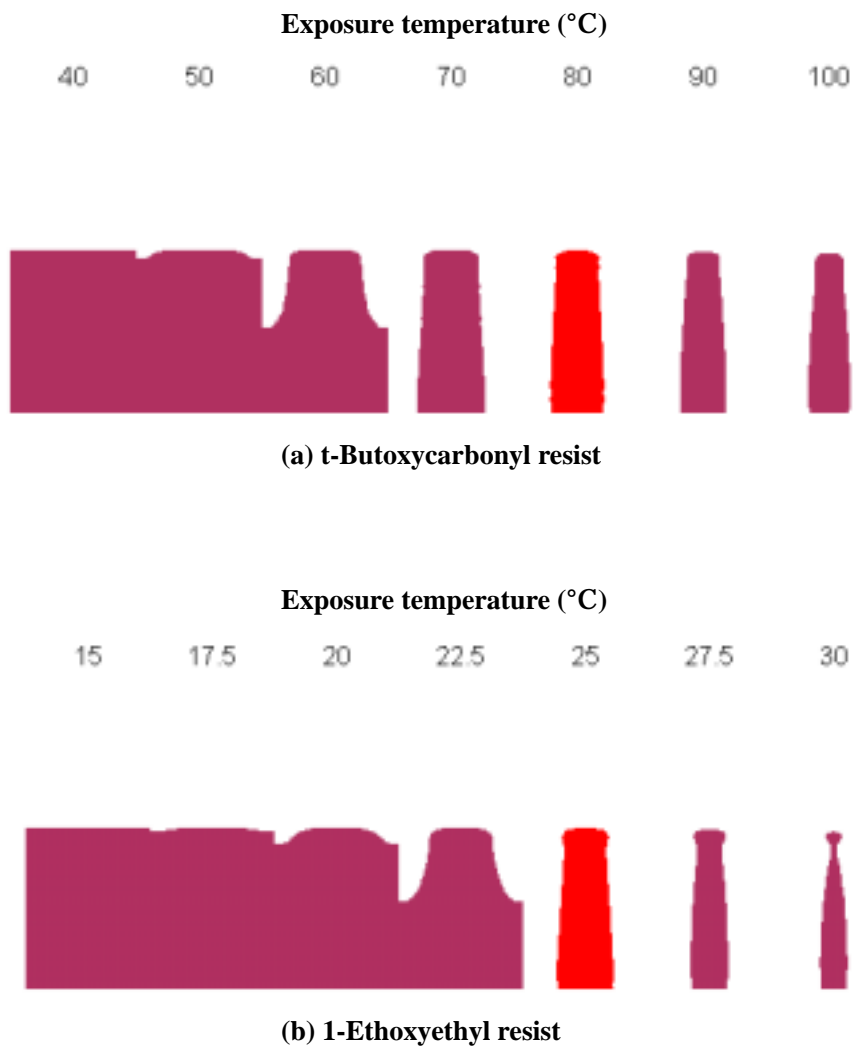


Fig.10 Simulation results for (a) t-butoxycarbonyl resist (prebake 90°C /60 s, L/S=0.25 $\mu$ m, exposure dose=7.00 mJ/cm<sup>2</sup>), and (b) 1-ethoxyethyl resist (prebake 90°C /60 s, L/S=0.25 $\mu$ m, exposure dose=1.73 mJ/cm<sup>2</sup>) without PEB.